Characterization of GOES-12 Aerosol Optical Depth Retrievals during ICARTT/INTEX-A

S. Kondragunta[1], P. Ciren[2], A. I. Prados[3], Y. Shinozuka[4], A. Clarke[4]

[1]NOAA/NESDIS Center for Satellite Applications and Research, 5200, Auth Road, Camp Springs, MD 20746

[2]QSS Inc., 5200 Auth Road, Camp Springs, MD 20746

[3]University of Maryland in Baltimore County/Joint Center for Earth Systems Technology, 5523 Research Park Drive, Baltimore, MD 21228

[4]University of Hawaii, Department of Oceanography, Honolulu, HI 96822

Abstract. Near real time movie loops of GOES aerosol optical depth (AOD) imagery were provided to guide aircraft and ship deployment during the ICARTT/INTEX-A field campaign. Quantitative post-mission data analysis showed that operational GOES AOD imagery provided accuracte spatial extent of pollution plumes despite residual cloud contamination in certain pixels. A new spatial variability threshold value of 0.1 for AOD standard deviation corresponding to eight surrounding pixels in a 3 X 3 box has been used to remove cloud contaminated pixels from GOES imagery; operational data were processed with a threshold value of 0.3. Our analysis shows that GOES AODs and ground-based AERONET observations agree well (35%) with a correlation coefficient (R) of 0.75 and a root mean squre (RMS) difference of 0.14. Similar agreement was observed between GOES AODs and aircraft AODs with a Rof 0.85 and a RMS difference of 0.14. Reprocessing GOES AODs with biomass burning aerosol model reduced the RMS difference to 0.1 but increased the bias with respect to AERONET observations (50%). In agreement with ground measurements, the two-month mean AODs were greater than 0.5 in the northeastern U.S. including Pennsylvania, Maryland, Virginia, West Virginia, New York and other neighboring regions. Time series analysis also shows excellent agreement between GOES and AERONET during June, July, and August for all 16 stations except Bondville in August. The good agreement between GOES/AERONET/aircraft AODs on different spatial and temporal scales demonstrates that GOES AODs are a good proxy to monitor pollution associated with urban/industrial sources and biomass burning events.

1. Introduction

A multi platform/sensor approach combining satellite, *in situ*, and model data is being increasingly considered to address science objectives such as determining the state of air quality over the United States (U.S.). Satellite data in particular are evolving as useful tools to track pollution ranging from regional to continental scales [*Al-Saadi et al.,* 2005; *Engel-Cox et al.,* 2004; *Hoff et al.,* 2005; *Wang and Christopher,* 2003]. The 2004 Intercontinental Chemical Transport Experiment-North America (INTEX-A) and NOAA's New England Air Quality Study (NEAQS) field campaigns under the International Consortium for Atmospheric Research on Transport and Transformation (ICARTT) provided an opportunity to assess the role of satellite data in extending spatial dimension to study problems such as contribution of long range transport to regional air quality. National Oceanic and Atmospheric Administration/National Environmental Satellite Data and Information Service (NOAA/NESDIS) provided near real time aerosol optical depth (AOD) product derived from Geostationary Operational Environmental Satellite (GOES-12) Imager to aid in the planning of aircraft and ship flight deployment. GOES AOD, available at 30-minute interval during the sunlit portion of the day and covering the CONtigous United States (CONUS) at 4 km X 4 km spatial resolution, were provided with one hour time lag to the field. GOES AOD data were integrated with other satellite imagery to determine how the weather systems were transporting pollutants and to determine the ideal location to sample with aircraft instrumentation [*Singh et al.,* this issue].

Accuracy of satellite retrieved aerosol optical depths and trace gases is not as good as measurements made from ground; satellite retrievals tend to have higher uncertainties. For aerosol optical depth retrievals, difficulties in modeling the aerosol type and contributions from surface lead to large uncertainties. Satellite retrievals such as GOES AODs that are performed in

near real time have additional sources of uncertainties such as those from sensor calibration errors, cloud contamination, and various other assumptions in the retrieval algorithm [*Knapp,* 2002; *Knapp,* 2005]. While careful screening and reprocessing can minimize retrieval errors due to surface reflectance, cloud contamination, and calibration errors, errors due to aerosol model assumptions are hard to reduce because it is not possible to dynamically choose an aerosol model that varies in space and time; current operational sensors such as the GOES Imager with only five channels (one visible, one near IR, three IR channels) do not have that capability.

The GOES AOD algorithm uses look-up tables (LUTs) created using a continental aerosol model (primarily consisting of water soluble sulfate and nitrate aerosol, soot, and dust), for which the single scattering albedo at 550 nm is ~0.89 [*Hess et al.,* 1998]. This includes assumptions about aerosol type, size distribution, and refractive index. However, variations in aerosol type and size can occur due to space and time dependent variations in sources of pollution (e.g., forest fires, urban/industrial, dust) resulting in uncertainties in retrieved AOD product. In this study, we analyze GOES AOD measurements with a specific focus on uncertainties related to the assumption of a single type of aerosol model across the whole CONUS. It should be noted that the assumption of aerosol model is for the whole column. In real atmosphere, aerosol type and size can vary as a function of height.

Evaluation of GOES AODs by comparing with AERosol RObotic NETwork (AERONET) and MODerate Imaging Spectrometer (MODIS) is an ongoing effort at NOAA/NESDIS [*Prados et al.,* 2006]. However, measurements of vertical extinction profiles, aerosol size distributions and type made during the field campaign provide an additional source of data to determine uncertainties in GOES AOD product for scenarios where atmospheric aerosol loading is dominated by different aerosol types.

In this study, we carry out post mission analysis and characterization of GOES AODs by comparing them with ground and aircraft AOD measurements made during the field campaigns in July and August of 2004. We present results on the assessment of the operational and reprocessed GOES AOD data on different temporal and spatial scales and the applicability of operational GOES AODs in supporting future field campaigns for air quality monitoring.

2. Data

2.1. GOES

The operational GOES AOD retrievals provided in near real time to the field campaign did not account for sensor calibration drift since the launch on GOES-12 in 2003. The operational data were also processed with GOES-8 look-up table. Since then, GOES AOD data were reprocessed with improved calibration (eliminating time dependent drift) and look-up table created using GOES-12 spectral response function. The impact of reprocessing on retrieved AODs is demonstrated using observations made on July 21, 2004 at 13 UTC. The two top panels of Figure 1 show operational and reprocessed GOES AOD maps for the northeastern U.S. respectively. The images show high optical depths corresponding to an event where smoke from forest fires was transported into the U.S. from Canada and Alaska. Operational AODs are higher, by up to 0.3 for this observation time period, compared to the reprocessed AODs although the spatial features in both products are similar (bottom left panel of Figure 1). The scatter plot between reprocessed and operational AOD clearly shows that operational AODs were about 11% higher than reprocessed values. On AOD scale, the impact of new calibration and look-up tables on retrieved AODs appears to be small for low aerosol loading (< 0.3). For example, the difference between operational and reprocessed AODs is calculated to be 0.0368

using the linear regression equation for an AOD of 0.3. As a percentage, however, this equals to 11%. Despite its uncertainties due to calibration errors, operational GOES AOD product met the needs of the field campaign which was primarily to aid in identifying aerosol plume locations and spatial variations in atmospheric aerosol loading. For quantitative applications such as verification of air quality forecasts issued during the campaign, there is a need to use accurate retrievals such as the reprocessed data. *Kondragunta et al.* (2006) used reprocessed GOES AOD data to evaluate National Weather Service developmental PM2.5 forecasts issued during the INTEX-A/NEAQS field campaign. Prior to using the reprocessed GOES AODs in their model verification study, *Kondragunta et al.* [2006] conducted extensive evaluation of GOES AOD data that is the basis for this paper.

2.2. AERONET

The level 1.5 (cloud-screened) AERONET AOD data for 17 stations mostly in the central and eastern U.S. corresponding to the INTEX –A domain with three in Canada were obtained from National Atmospheric and Space Administration (NASA) (http://aeronet.gsfc.nasa.gov) (Figure 2). The cloud-screening algorithm used to process the 2004 AERONET data has a tendency to flag high AODs as cloud contaminated [*Smirinov et al.,* 2000]. *Kaufman et al.* [2006] developed a new cloud-screening algorithm that corrects for this problem but the 2004 data have not yet been reprocessed with this algorithm. Thus, to avoid the removal of good data points from our analysis, we used level 1.5 data instead of level 2.0 which is cloud-screened and quality checked. AERONET AOD measurements are made using an automated combined spectral sunphotometer/sky radiometer, which can measure both the sky radiance and the attenuated direct sunlight using the same detector, optics, and special filters [*Holben et al.,*

1998]. AODs are measured at multiple wavelengths typically, at 331, 380, 441, 672, 873, and 1000 nm with an accuracy of ± 0.02 [*Holben et al.,* 1998]. We derived AODs for 550 nm by using the linear relationship between wavelength and AOD on a logartihmic scale.

2.3. Aircraft

Dry aerosol scattering extinction coefficients at 550 nm were measured with a nephelometer (model TSI 3563) in the visible channel along with dry aerosol size distributions from NASA's DC-8 aircraft [*Clarke et al.,* this issue]. Aircraft measurements of extinction profiles made using a nephlometer were integrated to obtain total column AODs. Coincident ambient relative humidity measurements were used to convert the dry scattering extinction coefficients to wet scattering extinction coefficients that are more representative of ambient aerosols. These adjustments were made based upon the scattering response to humidity change,f(RH), also measured on the DC-8 (Howell et al., 2006). The aircraft made about 72 flights during the campaign in July and August, 2004. After screening the satellite data as described in sections 2.1 and 3, we found 16 coincident aircraft vertical ascending and descending profiles with GOES data. Of these flights, some were transect flights over an area no greater than 2° X 2° longitude-latitude range and some were aircraft spirals confined to a small area within 50 km X 50 km. It should be noted that aircraft does not sample the lowest 500 m; values from 500 m are extrapolated to the surface. Aerosol absorption accounts for 0 – 10% of extinction and has been neglected in this study. For the spiral flights, coincident measurements of GOES AODs were obtained in two different ways. In the first approach GOES AOD pixels that fell into the grid (50 km X 50 km) corresponding to aircraft spiral were averaged and in the second approach GOES AOD pixels in a 3 X 3 box corresponding to the exact flight track were

averaged. Figure 3 shows an example of flight track overlaid over a composite spatial map of GOES AODs. GOES AOD composite was created from observations obtained within ±3 hours of aircraft flight time. An example of flight track overlaid over GOES AOD pixels underneath the flight track is given on XY plane on the top. In our comparisons of GOES AODs with aircraft measurements, we used the data averaged from pixels underneath flight track to exclude very high or very low AOD values that were in the box but not sampled by the aircraft. For example, there are high AODs observed by GOES south of the DC-8 profile. Since that part of the atmosphere was not measured by DC-8, inclusion of those data would have led to a positive bias between GOES and DC-8 AODs.

3. Matchup Criteria

For GOES vs AERONET and GOES vs MODIS, matchups were performed within 15 minutes of coincident observations. For each GOES observation time period (e.g., 1215 UTC), GOES AOD overpass data for each AERONET station was created by averaging AOD from the surrounding pixels in a 3 X 3 box (9 pixels). For AERONET data, observations coincident within 15 minutes of GOES observations are averaged. GOES AOD data before 11Z and after 21Z were not included in the analysis because of large solar zenith angle conditions. GOES AOD data for surface reflectivities less than 0.5% and greater than 15% were also not included in the analysis. An additional screen using a threshold value of 0.3 for AOD standard deviation corresponding to a 3 X 3 box (8 pixels) surrounding each pixel was developed. For GOES vs aircraft comparisons, we used integrated aircraft extinction profiles to calculate AOD. We used both extinction profiles reported for wet (ambient) aerosol and dry aerosol in our analysis; aerosol extinction profiles for wet (ambient) aerosol are derived by accounting for the effect of

relative humidity on dry aerosol and its scattering properties [*Howell et al.,* 2006]. No additional screens were applied for aircraft data and AERONET data.

4. Results and Discussion

4.1. GOES AOD Retrieval Evaluation

Figure 4 shows comparisons of reprocessed GOES AODs with those measured from a network of 17 AERONET stations within the domain in the U.S. confined to the ICARTT field campaign for June, July, and August 2004. For 4652 coincident observations, the correlation between the two datasets is 0.656 with a root mean square (RMS) difference of 0.185 associated with scatter in the data. In particular, GOES AODs are lower than AERONET by 26% (slope of the regression equation is 0.732). However, several of the outliers are the data points where GOES AODs are higher than AERONET AODs with few data points where AERONET is higher than GOES. Two potential reasons for GOES retrievals to be biased high can be residual cloud contamination and errors in surface retrieval that can translate into errors in retrieved AOD.

The GOES AOD retrieval algorithm (both operational and research version used for reprocessing) has multiple tests for identifying clouds and clear pixels contaminated with clouds. The tests originally developed for Advanced Very High Resolution Radiometer (AVHRR) by *Stowe et al.* [1999] were modified and adapted for the GOES Imager [*Knapp et al.,* 2005]. An additional screening test that relies on spatial variability in retrieved AOD is used to remove cloud contaminated pixels. In this test, for every pixel, average AOD and its standard deviation are computed from the surrounding 8 pixels in a 3 X 3 box. Any pixel for which AOD standard deviation is greater than 0.3 or number of clear pixels in a 5 X 5 box (i.e. surrounding 24 pixels)

are fewer than 15, is flagged as a bad retrieval. Despite this screening test, some pixels may have residual cloud contamination leading to high bias in GOES AODs.

To test if the outliers (points where GOES AODs are higher than AERONET) are due to residual cloud contamination, we carried out analysis similar to *Martins et al.* [2002] to identify residual cloud contamination. Frequency distribution of GOES 3 X 3 AOD standard deviation showed that the distribution peaks between 0.1 and 0.2 (Figure 5). AOD standard deviation in a 3 X 3 box can be high for certain pixels due to either cloud contamination of some pixels or errors in surface reflectance retrieval or true variability in AOD over small spatial scales. Without multiple ground-based observations over a small spatial domain, one way of determining this threshold is to investigate the bias between GOES and AERONET AOD as a function of AOD standard deviation (Figure 6). For the three month time period we investigated, our analysis shows that bias increases with increasing AOD standard deviation. When the standard deviation is smaller than 0.1, the bias is closer to zero and data points are tightly aligned near the zero offset line. As AOD standard deviation increases, the data points diverge from the zero line spreading farther apart. Using this information along with Figure 5, we refined the screening test and changed the AOD standard deviation threshold from 0.3 to 0.1 and the number of clear pixels in the 5 X 5 box to be equal to 25 instead of greater than 15. After the data were screened using this new test for residual cloud contamination, the correlation between GOES and AERONET AODs improved substantially. With the new cloud screening test, GOES and AERONET AODs have a correlation coefficient of 0.73, RMS difference of 0.14, and near zero intercept (Figure 7). Note that RMS difference without the new test is 0.185 (Figure 4). While most of the data points with errors due to cloud contamination along the cloud edges and in the vicinity of clouds are flagged as bad retrievals with this new cloud screening test, pixels near the

edge of an aerosol plume boundary where AOD is likely to vary, will also be flagged as bad data. Although few outliers where AERONET AOD is much higher than GOES AOD still remain even after the new screening test is used, most of the outliers and noisy data points have been removed. Most of the remaining outliers are from Bondville station. Analysis of AERONET data from Bondville station shows that while the Level 1.5 data for July 2004 are nearely identical to Level 2.0, Level 1.5 August data have high AODs that have been screened in Level 2.0 data indicating that AERONET data are in error, not GOES. It should be noted that the tighter screening reduced the number of coincident observations by 67% for this time period (number of matchups reduced from 4652 to 2839).

We also investigated for the sources of uncertainties in GOES AOD retrievals due to aerosol model assumptions. The summer 2004 was dominated by long range transport of smoke [*Fulberg et al.,* this issue]. Nearly 3.2 million acres in Canada and 3.4 million acres in Alaska burned releasing huge amounts of smoke into the atmosphere, according to National Interagency Fire Center (NIFC). Weather patterns were such that in mid-July, the smoke was transported over the U.S. [*Fulberg et al.,* this issue]. Although smoke was predominantly over the central U.S., east of Ohio River Valley region, sulfate aerosols were also present in the Planetary Boundary Layer (PBL) with smoke aerosols aloft [*Kondragunta et al.,* 2006; *Clarke et al.,* this issue]. While the true nature of aerosol mixture is difficult to determine as a function of space and time, to account for the presence of smoke aerosol in our retrievals, we reprocessed the GOES-12 data using a biomass burning aerosol model assuming that all atmospheric aerosol loading is due to smoke [*Kahn et al.,* 2001]. The various components of this model are carbonaceous (54%), sulfate (25%), dust (12%), and black carbon (9%) making this aerosol mixture highly absorbing with a single scattering albedo at 550 nm of 0.78. Monitoring data

from Environmental Protection Agency (EPA) Speciation Trends Network (STN) indicate that in the eastern part of the U.S. carbonaceous and sulfate aerosols were nearly equal [*U.S. Environmental Protection Agency,* 1997]. Along with the long-range transport of smoke, a regional-scale sulfate event developed over the eastern U.S. resulting in an aerosol mixture which was probably not as absorbing as the biomass burning aerosol model we used [*Hennigan et al.,* this issue].

Figure 8 shows the correlation between GOES AODs reprocessed with LUTs created from the biomass burning aerosol model and AODs from 17 AERONET stations. The correlation coefficient is 0.72 and RMS difference is 0.1. While the correlation coefficient value for the correlation between GOES AOD processed with smoke aerosol model and AERONET AODs is nearly identical to the one where GOES AODs were processed with continental aerosol model, the RMS value and slope are different. Slope is closer to unity (~0.70) for continental aerosol model compared to the smoke aerosol model (~0.55). Root Mean Square difference between GOES and AERONET AODs is smaller for the smoke aerosol model compared to the continental aerosol model by 28% (0.14 vs 0.1). This is because the use of smoke aerosol model resulted in lowering the magnitude of GOES AOD values for situations when aerosol loading was high and perhaps consisting of mostly smoke aerosol. As a result, the scatter in the data (outliers) decreased and improved the RMS value. Table 1 lists correlation coefficients, RMS differences, and slopes for each of the 17 individual AERONET stations for both smoke and continental aerosol models. Results are consistent between all stations with correlation being similar but with improved RMS values for GOES AODs retrieved using a smoke aerosol model versus continental aerosol model. Slopes of the regression equation between GOES and AERONET AODs vary from station to station for a given aerosol model. However, for almost

any particular station, slope is closer to 1.0 for a continental aerosol model than for the smoke model. Most satellite aerosol retrieval algorithms choose an aerosol model *a priori* using different approaches. For example, the MODIS algorithm chooses its models depending on the geographical region and Multi-angle Imaging SpctroRadiometer (MISR) algorithm chooses its models based on climatology built from global transport model [*Kahn et al.,* 2001; *Remer et al.,* 2005]. An ideal situation would be for satellite radiances to provide the information on aerosol type so an appropriate model can be dynamically chosen. Currently that capability is limited except for instruments such as MODIS whose measurements can provide the information to distinguish between dust and non-dust aerosols [*Remer et al.,* 2005]. Errors in assumptions of aerosol models lead to systematic biases in AOD retrievals. However, these biases can vary in space and time depending on the actual aerosol type and magnitude of aerosol loading (Table 1). Having an aerosol model that accounts for a wide variety of aerosols such as a continental aerosol model will prevent the algorithm from being tuned for episodic cases such as biomass burning or dust storms. This is further illustrated in the time series plots of daily mean GOES AOD and AERONET AOD averaged over all 17 stations (Figure 9). The black line is for AERONET, blue line for GOES AOD with smoke aerosol model, and red line is for GOES AOD with continental aerosol model. There is a good agreement between the two datasets in the time series plot when continental aerosol model is used especially during the time period between days 200 and 210 (July 18 – July 28, 2004) when the agreement between GOES and AERONET is poor for the smoke aerosol model. This time period also corresponds to the regional-scale sulfate event in the eastern U.S. The smoke model is more absorbing and appears to have over compensated the extinction properties of the aerosol mixture. While the correlation between AERONET and GOES AOD is similar for both aerosol models, the slopes are drastically

different (also see Table 1). In general, AODs derived using the smoke aerosol model have a lower slope when compared to AERONET AODs indicating that the bias is larger. Thus the choice of aerosol model, unless satellite observations provide that information, will continue to be a challenge for retrieving aerosol optical depths.

Aircraft observations provide a good constraint for satellite retrievals. These profiles were adjusted to the ambient conditions based upon measured f(RH) and integrated to obtain total column optical depth. Aircraft data provide useful information on the vertical location of the plume. In this study, we assumed that plumes above 3 km are smoke and aerosol loading below that is due to urban/industrial haze, consistent with most observations of plumes on the DC-8 during INTEX-NA [*Clarke et al.,* this issue]. Figure 10 (top panel) shows correlation between GOES AODs with measurements made by the DC-8 aircraft. AODs from GOES pixels along the aircraft flight track were averaged, after using the screening criteria described in section 2.1 and the new spatial variability test described in section 4.1. We compared DC-8 AODs for both wet (i.e. ambient) aerosol shown in blue and dry aerosol shown in red with GOES AODs. Agreement between GOES and DC-8 AODs is better, as expected, for ambient (wet) aerosol with correlation coefficient of 0.85 and RMS difference of 0.14. We also tagged each matchup data point shown in Figure 10 (top panel) into “aloft” or “not aloft” by manually analyzing the DC-8 scattering extinction profiles to identify if aerosols were above the PBL or in PBL. We used the altitude cutoff of 3 km to define PBL height. We attributed the presence of aerosols aloft to long-range transport of smoke and assumed that aerosols within 3 km to be due to regional scale urban/industrial pollution. Figure 10 (bottom panel) shows correlation between GOES and DC-8 AODs for wet aerosol where data points are clearly identified as aerosols aloft (black) or not aloft (blue). There is no difference in correlation between GOES and DC-8

AODs when aerosols are aloft or in the boundary layer below 3 km. Additionally, repeating the analysis by replacing data points identified as "aloft aerosols" with GOES AOD data retrieved using biomass burning aerosols did not change the correlation significantly. Although the number of matchups was only 17, this preliminary analysis suggests that the performance of GOES AOD retrieval algorithm is similar for conditions where aerosol is in the PBL or in the free troposphere. Additional analysis using data from other instruments on aircrafts will be carried out in the future to confirm this finding.

4.2. Spatial and Temporal Patterns in Atmospheric Aerosol Loading during INTEX-NA

The summer of 2004 was effected by the long range transport of smoke from biomass burning in Canada and Alaska resulting in elevated aerosol optical depths over the mid-western and eastern U.S (Figure 11). The most intense part of the smoke transport took place between July 16 and July 22, 2004 due to favorable weather patterns [*Fulberg et al.,* this issue] resulting in elevated aerosol loading (> 0.1) throughout the domain with highest aerosol loading (> 0.5) over the eastern states Pennsylvania, Maryland, Virginia, West Virginia, and North Carolina. High aerosol loadings were also observed over Georgia and over the coastal region off of Maine. Time series of daily mean AOD values from ten AERONET stations and corresponding GOES AOD data show that high aerosol loading was present from days 198 to 204 (July 16 to July 22) and in mid-August (beginning day 230) (Figure 12). Temporal variations in both GOES and AERONET AOD data matched very well with both datasets capturing the high and low AODs during this time period well. The 17 AERONET stations used in this analysis are spread over the central and eastern U.S. and are not geographically restricted to one region. Thus, AOD data from GOES and sunphotometer corresponding to these sites represents the spatial variability observed in the study region. Elevated aerosol loading in the eastern U.S. during summers is not

uncommon. High pressure systems conducive for photochemical smog very commonly lead to elevated ozone and aerosol concentrations in the eastern U.S. when transport brings emissions from power plants in the Ohio River Valley region [*Taubman et al.,* 2004; *Marufu et al.,* 2004]. A similar situation led to a regional-scale sulfate haze event leading to elevated aerosol amounts in addition to the long range transport of smoke from fires in Alaska and Canada [*Kondragunta et al.,* 2006). Satellite data can neither distinguish between these coincident pollution events nor can they provide information on the vertical location of the plume. Thus, in absence of *in situ* such as aircraft observations, we cannot positively conclude how much of this elevated aerosol loading is due to long-range transport and how much is due to local regional haze associated with a sulfate event. Barring errors associated with chemistry, physics, and dynamics, Community Multiscale Air Quality Model (CMAQ) simulations of AOD for this time period show that contributions can be as large as 100% (i.e., all observed AOD is due to smoke) or as small as 40% (i.e., 60% of observed AOD is due to industrial pollution) [*Kondragunta et al.,* 2006]. Aircraft observations indicate that while the smoke was aloft, the sulfate event was confined to below 3 km [*Clarke et al.,* this issue]. Aircraft measurements of aerosol properties during the INTEX-NA time period, in the horizontal (transect flights) and vertical (spiral flights), were mostly made in this region covered by high aerosol optical depths providing an opportunity to evaluate GOES AODs over a wide range of values and aerosol types (industrial/urban aerosol vs smoke aerosol). The agreement between DC-8 measured and GOES AODs retrieved using continental aerosol model shows that satellite data have captured the variability in atmospheric AOD over multiple days and different observation time (different viewing conditions).

5. Conclusions

The ICARTT/INTEX-A/NEAQS field campaigns not only facilitated the use of satellite imagery in providing on-the fly qualitative spatial look of pollution events but also provided useful ground and aircraft data to quantitatively evaluate satellite retrievals as part of post mission data analysis. In this study, we characterized GOES-12 AODs that were provided to support the ICARTT/INTEX-A/NEAQS field campaign by comparing with AERONET and NASA DC-8 AOD measurements. Initial analysis showed good agreement with GOES-12 and AERONET AODs with a correlation coefficient of 0.656. However, several outliers in the scatter plot between GOES-12 and AERONET AODs resulted in a higher RMS value (0.185). Further analysis of the data showed that the outliers were probably due to residual cloud contaminations which were objectively removed using a new spatial variability test. After screening the data with the new test, correlation between GOES and AERONET AODs improved (R = 0.75) and RMS value decreased (0.14). GOES AODs also showed very good agreement with DC-8 measurements with a correlation coefficient of 0.85 and RMS value of 0.14. The use of biomass burning aerosol model to represent smoke transported from Canada and Alaska into the U.S. in GOES AOD retrieval algorithm introduced a bias in the retrievals although the RMS difference between AERONET and GOES AODs decreased. For most stations studied, the slope for the regression between GOES and AERONET was closer to unity when continental aerosol model was used as opposed to biomass burning aerosol. The use of biomass burning aerosol model is perhaps best suited for the central U.S. but not for the eastern U.S. where in addition to long range transport of smoke there was a regional scale sulfate pollution in the boundary layer, below 3 km. A combination of biomass burning aerosol model

and continental aerosol model would be a good choice for the eastern U.S. and in our future studies, we will consider that approach.

On different spatial and temporal scales, GOES AODs captured the variability well. Spatially, two-month mean AODs were greater than 0.5 in the northeastern U.S. including Pennsylvania, Maryland, Virginia, West Virginia, New York and other neighboring regions. This is in agreement with high AODs observed from satellites and ground observations in the summer in the northeastern U.S. Time series analysis shows excellent agreement between GOES and AERONET during June, July, and August except for Bondville station in August. Additional analysis is needed to fully understand the discrepancies between GOES and AERONET AODs for Bondville station. The good agreement between GOES/AERONET/DC-8 AODs on different spatial and temporal scales, for the domain we studied, demonstrates that GOES AODs capture variability in atmospheric aerosol loading well and are a good proxy to monitor pollution associated with urban/industrial sources and biomass burning events. It should be noted, however, that the domain we studied provides ideal observing conditions (low surface reflectivity, high aerosol loading) for retrieving AODs from satellites. Recently concluded INTEX-B campaign and summer 2006 TexAQS (TexAS Air Quality Study) will provide data over the south central and western regions to characterize GOES AOD retrievals over dry and arid regions of the U.S. where surface reflectances are high and conditions are not favorable for satellite retrievals.

Analysis carried out in this study is our initial attempt to characterize the performance of GOES AOD retrieval algorithm. We showed that, despite errors in the order of ~11%, operational GOES AOD imagery provided useful information and aided the INTEX-A/NEAQS mission team. Post mission data analysis has allowed us to investigate errors associated with

cloud contamination and aerosol model assumptions, leading to a conclusion that the use of continental aerosol model in our operational and research algorithm is better than an event-based specific aerosol model such as a biomass burning aerosol model. In future studies, we will carry out closure studies on individual cases where both aircraft extinction profiles and aerosol size distributions as a function of height are available.

Acknowledgements. This work was supported in part by NOAA's GIMPAP and G-PSDI programs. The authors would like to acknowledge C. McNaughton and S. Howell of University of Hawaii for assistance in processing NASA DC-8 measurements, J. J. Szykman of Environmental Protection Agency, C. Kittaka of Science Applications International Corporation, and T. J. Kleespies of NOAA/NESDIS for useful discussions. The authors would also like to thank Principal Investigators (PIs) of AERONET stations for making their data available through NASA. Although this work has been internally reviewed, views expressed in this paper are those of authors and do not reflect any position of Government or National Oceanic and Atmospheric Administration.

References

Al-Saadi, J., et al. (2005), Improving national air quality forecasts with satellite aerosol observations, *Bulletin of American Meteorological Society*, *86,* 1249-1261.

Clarke, A. D., V. Kapustin, S. G. Howell, C. S. McNaughton, Y. Shinozuka, B. Anderson, J. Dibb, Aerosol from biomass burning and regional pollution over North America during INTEX-NA: Humidity response and the wavelength dependence of scattering and absorption , submitted, this issue.

Engel-Cox, J., C. H. Holloman, B. W. Coutant, R. R. Hoff (2004), Qualitative and quantitative evaluation of MODIS satellite sensor data for regional and urban scale air quality, *Atmos. Environ., 38,* 2495-2509.

Fuelberg, H., M. J. Porter, C. M. Kiley, and D. Morse, Meteorological conditions and anomalies during INTEX-NA, submitted, this issue

Hess, M., P. Koepke, I. Schult (1998), Optical Properties of Aerosols and Clouds: The software package OPAC, *Bulletin of American Meteorological Society, 79,* 831-844.

Hoff, R. M., S. P. Palm, J. A. Engel-Cox, J. Spinhirne (2005), GLAS long-range transport observation of 2003 California forest fire plumes to the northeastern US, *Geophys. Res. Lett., 32,* L22S08, doi:10.1029/2005GL023723

Hennigan, C., S. Sandholm, S. Kim, R. Stickel, G. Huey, R. Weber, Influence of Ohio River Valley Emissions on Fine Particle Sulfate Measured from Aircraft over Large Regions of the Eastern U.S. and Canada during INTEX-NA, submitted, this issue

Holben, B. N., T. F. Eck, I. Slustsker, D. Tanre, J. P. Buis, A. W. Setzer, E. F. Vermote, Y. J. Kaufman, T. Nakajima, F. Lavenu, I. Jankowiak, A. Smirnov (1998), AERONET: A federated instrument network and data archive for aerosol characterization, *Remote Sensing of Environment, 66,* 1-16.

Howell, S. G., A. D. Clarke, Y. Shinozuka, V. Kapustin, C. S. McNaughton, B. J. Huebert, S. J. Doherty, and T. L. Anderson (2006), Influence of relative humidity upon pollution and dust during ACE-Asia: Size distributions and implications for optical properties, *J. Geophys. Res., 111,* D06205, doi:10.1029/2004JD005759.

Kaufman, Y. J., G. P. Gobbi, and I. Koren (2006), Aerosol climatology using a tunable spectral variability cloud screening of AERONET data, *Geophys. Res. Lett., 33,* L070817, doi:10.1029/2005GL025478.

Kahn, R., P. Banerjee, and D. McDonald (2001), Sensitivity of multiangle imaging to natural mixtures of aerosols over ocean, *J. of Geophys. Res., 106,* D16, 18219-18238.

Knapp, K. (2002), Quantification of aerosol signal in GOES-8 visible imagery over the U.S., *J. of Geophys. Res., 107,* 10.1029/2001JD002001.

Knapp, K. E., Frouin, R., Kondragunta, S., and A. I. Prados (2005), Towards aerosol optical depth retrievals over land from GOES visible radiances: Determining surface reflectance, *Int. J. of Rem. Sens., 26,* no. 18, 4097-4116.

Kondragunta, S., P. Lee, J. McQueen, C. Kittaka, A. Prados, P. Ciren, I. Laszlo, B. Pierce, R. Hoff, J. Szykman (2006), Air Quality Forecast Verification using Satellite Data, *J. of Appl. Met., submitted.*

Remer, L. A., Y. J. Kaufman, D. Tanre, S. Mattoo, D. A. Chu, J. V. Martins, R-R. Li, C. Ichoku, R. C. Levy, R. G. Kleidman, T. F. Eck, E. Vermote, B. N. Holben (2006), The MODIS Aerosol Algorithm, Products and Validation, *J. of Atmos. Sci., in press*

Smirnov, A., B. N. Holben, T. F. Eck, O. Dubovik, and I. Slutsker (2000), Cloud screening and quality control algorithms for the AERONET database, *Rem. Sens. Env., 73,* 337-349.

Prados, A. I., S. Kondragunta, I. Laszlo, P. Ciren, K. Knapp (2006), The GOES Aerosol/Smoke Product (GASP) over North America: Comparisons to AERONET and MODIS, *J. of Geophys. Res., submitted.*

Stowe, L. L., P. A. Davis, and E. P. Mcclain (1999), Scientific basis and initial evaluation of the CLAVR-1 global clear/cloud classification algorithm for the Advanced Very High Resolution Radiometer, *J. of Atm. and Oce. Tech., 16,* 651-681.

U.S. Environmental Protection Agency (1997). Revised Requirements for Designation of Reference and Equivalent Methods for PM2.5 and Ambient Air Quality Surveillance for Particulate Matter; Final Rule. *Federal Register, 62 (38763).*

Marafu, L. T., B. F. Taubman, B. Bloomer, C. A. Piety, B. Doddridge, J. W. Stehr, and R. R. Dickerson (2004), The 2003 blackout over eastern North America: An accidental experiment in air chemistry, *Geophys. Res. Lett., 31*(13), L13106.

Martins, J. V., D. Tanre, L. A. Remer, Y. J. Kaufman, S. Mattoo, and R. Levy (2002), MODIS cloud screening for remote sensing of aerosol over oceans using spatial variability. *Geophys. Res. Lett.*, 29, doi: 10.1029/2001GL01352.

Taubman, B. F., T. Marafu, C. A. Piety, B. G. Doddridge, J. W. Stehr, and R. R. Dickerson (2004), Airborne characterization of the chemical, optical, and meteorological properties, and origins of a combined ozone/haze episodes over the eastern U.S., *J. of Atmos. Sci., 61,* Issue 14, P1781.

Wang, J. and S. Christopher (2003), Intercomparison between satellite-derived aerosol optical thickness and PM2.5 mass: Implications for air quality studies, *Geophys. Res. Lett., 30,* 21, 2095, doi:10.1029/20034L018174.

Singh, H. B., W. Brune, J. Crawford, and D. Jacob, Overview of the Summer 2004 Intercontinental Chemical Transport Experiment-North America (INTEX-A), *this issue, submitted.*

Figure 1: Difference between reprocessed and operational GOES-12 AOD data for 13Z July 21, 2004. Top left panel shows reprocessed AOD with improved calibration and accurate Look-Up Table (LUT), top right panel shows operational data, bottom left panel shows difference in AOD between reprocessed and operational data, and bottom right panel shows correlation between reprocessed and operational AOD. Note that plume location is the same in both operational and reprocessed data. Differences up to 0.3 are observed in the thick of the plume. Reprocessed AODs are lower than operational AODs. In the bottom right panel, white line is for regression line and black line is for 1:1 line.

Figure 2: A map of available AERONET stations with routine AOD measurements. Stations within the blue box were used in this study.

Figure 3: Example of an aircraft extinction profile overlaid on GOES AOD composite. The vertical line is the extinction profile of aircraft (color scale for this profile is shown on bottom left). GOES quality screened AOD composite is shown as a 2-D field (XY plane). The gray lines on the XZ and YZ planes are projected flight track. Mean GOES AOD in a box of 3 by 3 pixels on the projected flight track on XY plane is shown at the top.

Figure 4: Correlation between GOES aerosol optical depth (AOD) and AODs measured from a network of 17 AERONET stations. Level 1.5 AERONET data were used. Matchup criteria were coincident measurements within 15 minutes. GOES AOD data were excluded if surface reflectance was smaller than 0.5% or greater than 15%, AOD standard deviation in 3 X 3 box

was greater than 0.3, and number of cloud-free pixels in the 5 X 5 box were less than 15. Solid line is the 1:1 line and the dashed line is for the derived regression equation.

Figure 5: Frequency distribution of AOD standard deviation computed using AODs from 8 pixels in a 3 X 3 box surrounding a particular pixel. Data from July 21, 2004 2215Z were used in the analysis shown in the figure. Data from other days and other time periods show similar distribution.

Figure 6: Relationship between GOES and AERONET AOD bias as a function of AOD standard deviation. AOD standard deviation was computed using AODs from 8 pixels surrounding a particular pixel. Bias increases with increasing AOD standard deviation indicating residual cloud contamination. The vertical bars are 1-σ variability over the mean AOD standard deviation.

Figure 7: Correlation between GOES aerosol optical depth (AOD) and AODs measured from a network of 17 AERONET stations. Level 1.5 AERONET data were used. Matchup criteria were coincident measurements within 15 minutes. GOES AOD data were excluded if surface reflectance was smaller than 0.5% or greater than 15%, AOD standard deviation in 3 X 3 box was greater than 0.1, and number of cloud-free pixels in the 5 X 5 box were less than 25. Solid line is the 1:1 line and the dashed line is for the derived regression equation.

Figure 8: Same as figure 7 but for smoke aerosol model.

Figure 9: Time series of average daily mean GOES AOD overpass data from 17 AERONET stations. AERONET data are shown in black, GOES data processed with continental aerosol model in red, and GOES AOD data processed with smoke aerosol model in blue. Data begin on July 1, 2004 and end on August 31, 2004.

Figure 10: Ccorrelation between GOES and DC-8 aircraft measured AOD. Top panel is for wet and dry aerosols and bottom panel is for aerosols aloft vs not aloft.

Figure 11: Mean aerosol optical depth for July – August, 2004 obtained from the visible channel of the GOES-12 Imager. AOD measurements are reported for 550 nm although the visible channel is a broad band covering 0.52 – 0.72 μm.

Figure 12: Time series of daily mean AOD from AERONET (red), GOES with continental aerosol model (blue), and GOES with smoke aerosol model (black) for eight different stations in the central and eastern U.S.

Table 1: Correlation between AERONET and GOES AODs

Wallops	0.820	0.92	0.116	0.809	0.685	0.09

Station	*R*	*Slope*	*RMS*	*R*	*Slope*	*RMS*
	(Continental Aerosol Model)			*(Smoke Aerosol Model)*		
Wallops	0.820	0.92	0.116	0.809	0.685	0.09
Bondville	0.36	0.176	0.130	0.411	0.143	0.096
Brookhaven	0.826	1.023	0.13	0.846	0.813	0.096
Cartel	0.715	0.630	0.103	0.666	0.459	0.087
CCNY	0.842	0.920	0.100	0.825	0.738	0.086
Columbia, SC	0.270	0.310	0.150	0.231	0.209	0.119
COVE	0.879	0.930	0.089	0.863	0.814	0.084
Dry_Tortugas	0.606	0.896	0.050	0.604	0.923	0.054
Egbert	0.812	0.779	0.1	0.818	0.581	0.073
GSFC	0.811	0.996	0.138	0.797	0.715	0.104
Howland	0.449	0.414	0.121	0.384	0.285	0.1
Kellog_LTER	0.226	0.122	0.136	0.233	0.102	0.111
KONZA	0.458	0.767	0.089	0.456	0.597	0.069
MD_ScienceCenter	0.751	0.84	0.135	0.744	0.633	0.104
MVCO	0.791	0.572	0.136	0.812	0.470	0.104
SERC	0.819	0.942	0.136	0.801	0.69	0.130
Walker_Branch	0.516	0.40	0.108	0.528	0.319	0.084
Wallops	0.820	0.92	0.116	0.809	0.685	0.09

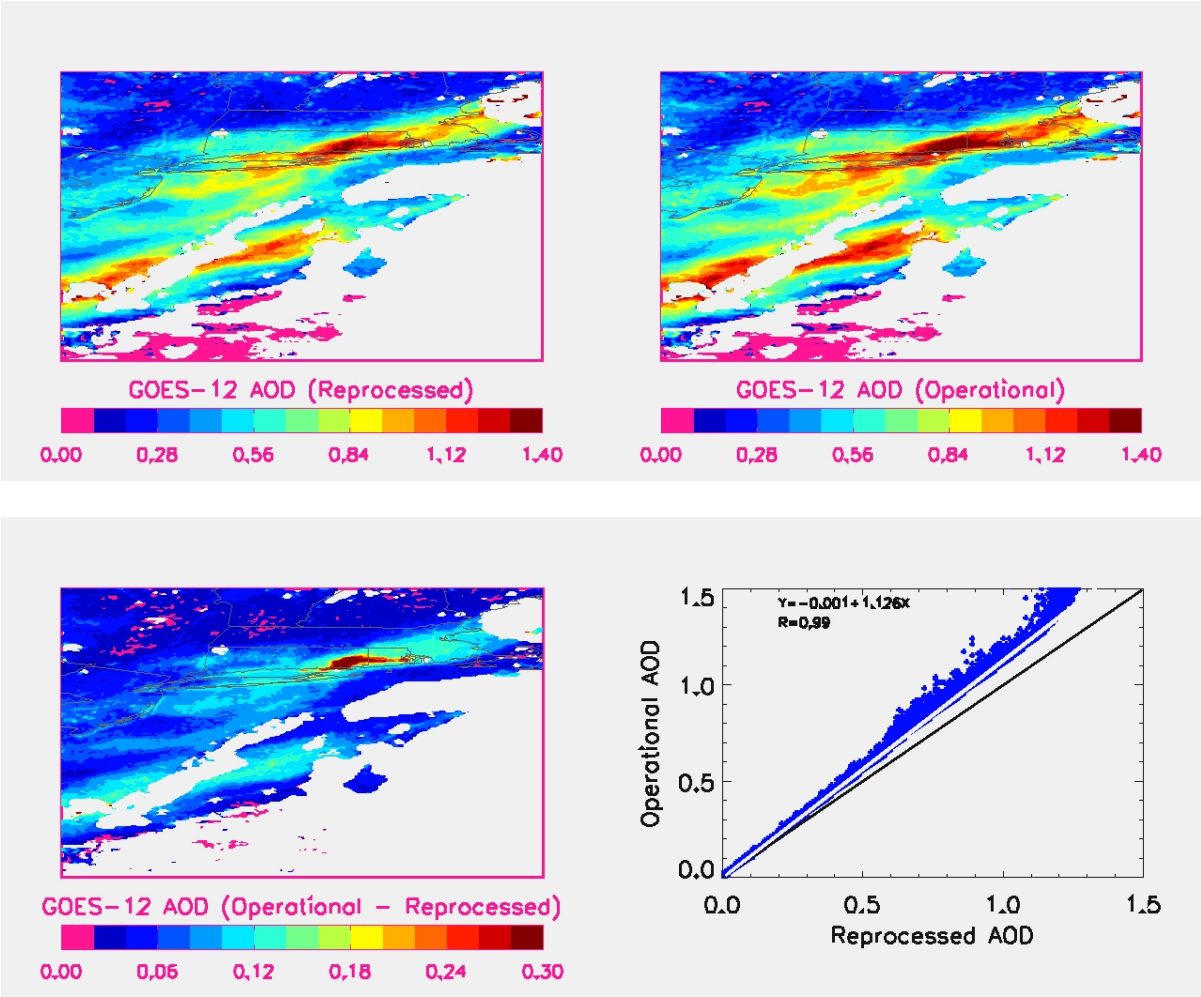

Figure 1: Difference between reprocessed and operational GOES-12 AOD data for 13Z July 21, 2004. Top left panel shows reprocessed AOD with improved calibration and accurate Look-Up Table (LUT), top right panel shows operational data, bottom left panel shows difference in AOD between reprocessed and operational data, and bottom right panel shows correlation between reprocessed and operational AOD. Note that plume location is the same in both operational and reprocessed data. Differences up to 0.3 are observed in the thick of the plume. Reprocessed AODs are lower than operational AODs. In the bottom right panel, white line is for regression line and black line is for 1:1 line.

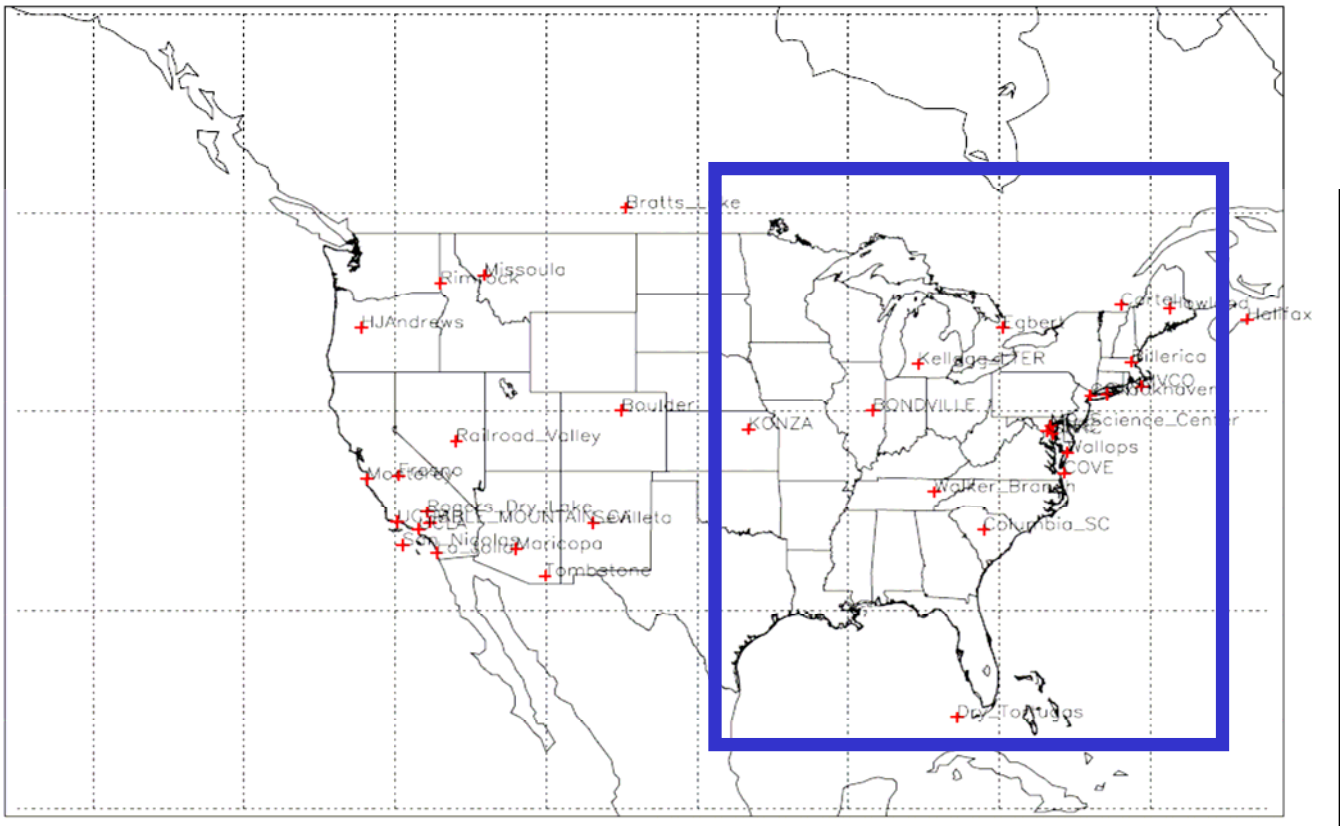

Figure 2: A map of available AERONET stations with routine AOD measurements. Stations within the blue box were used in this study

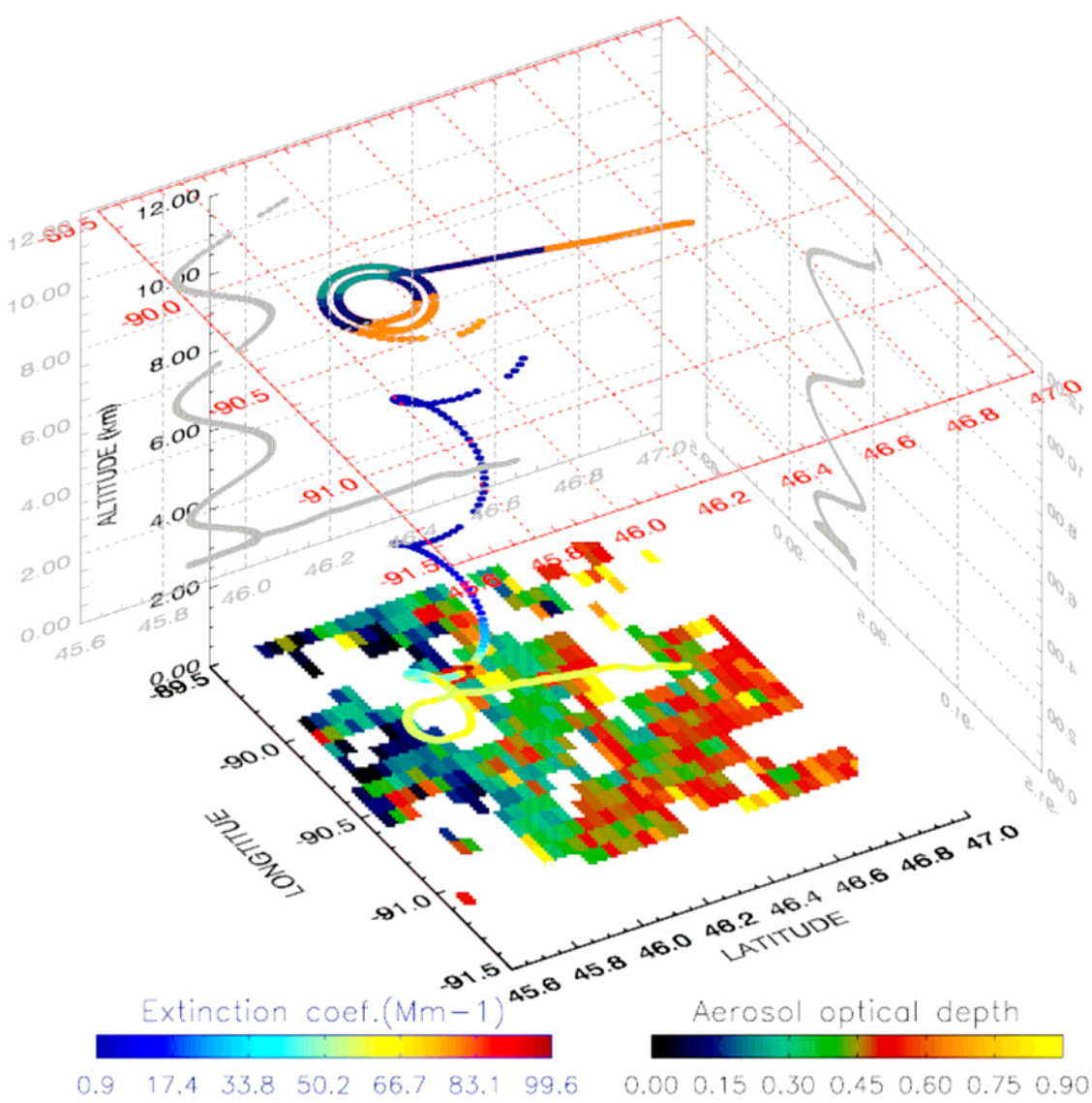

Figure 3: Example of an aircraft extinction profile overlaid on GOES AOD composite. The vertical line is the extinction profile of aircraft (color scale for this profile is shown on bottom left). GOES quality screened AOD composite is shown as a 2-D field (XY plane). The gray lines on the XZ and YZ planes are projected flight track. Mean GOES AOD in a box of 3 by 3 pixels on the projected flight track on XY plane is shown at the top.

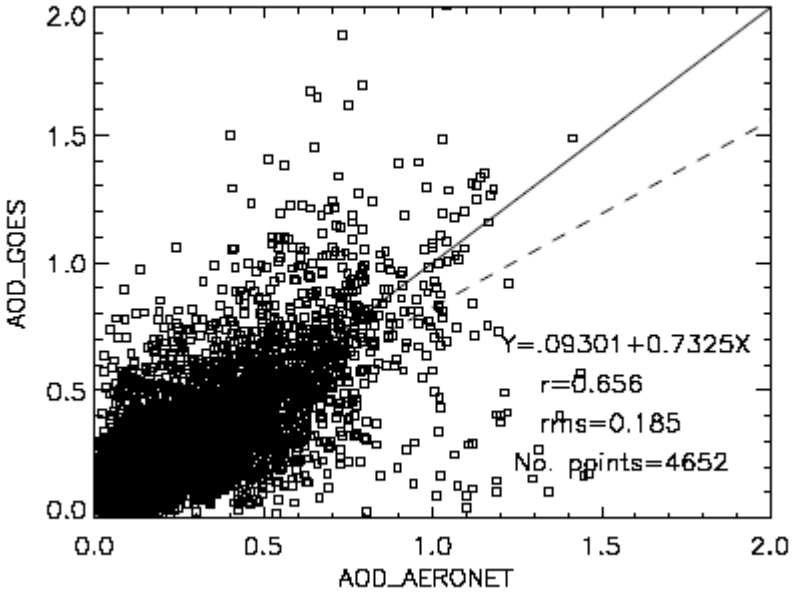

Figure 4: Correlation between GOES aerosol optical depth (AOD) and AODs measured from a network of 17 AERONET stations. Level 1.5 AERONET data were used. Matchup criteria were coincident measurements within 15 minutes. GOES AOD data were excluded if surface reflectance was smaller than 0.5% or greater than 15%, AOD standard deviation in 3 X 3 box was greater than 0.3, and number of cloud-free pixels in the 5 X 5 box were less than 15. Solid line is the 1:1 line and the dashed line is for the derived regression equation.

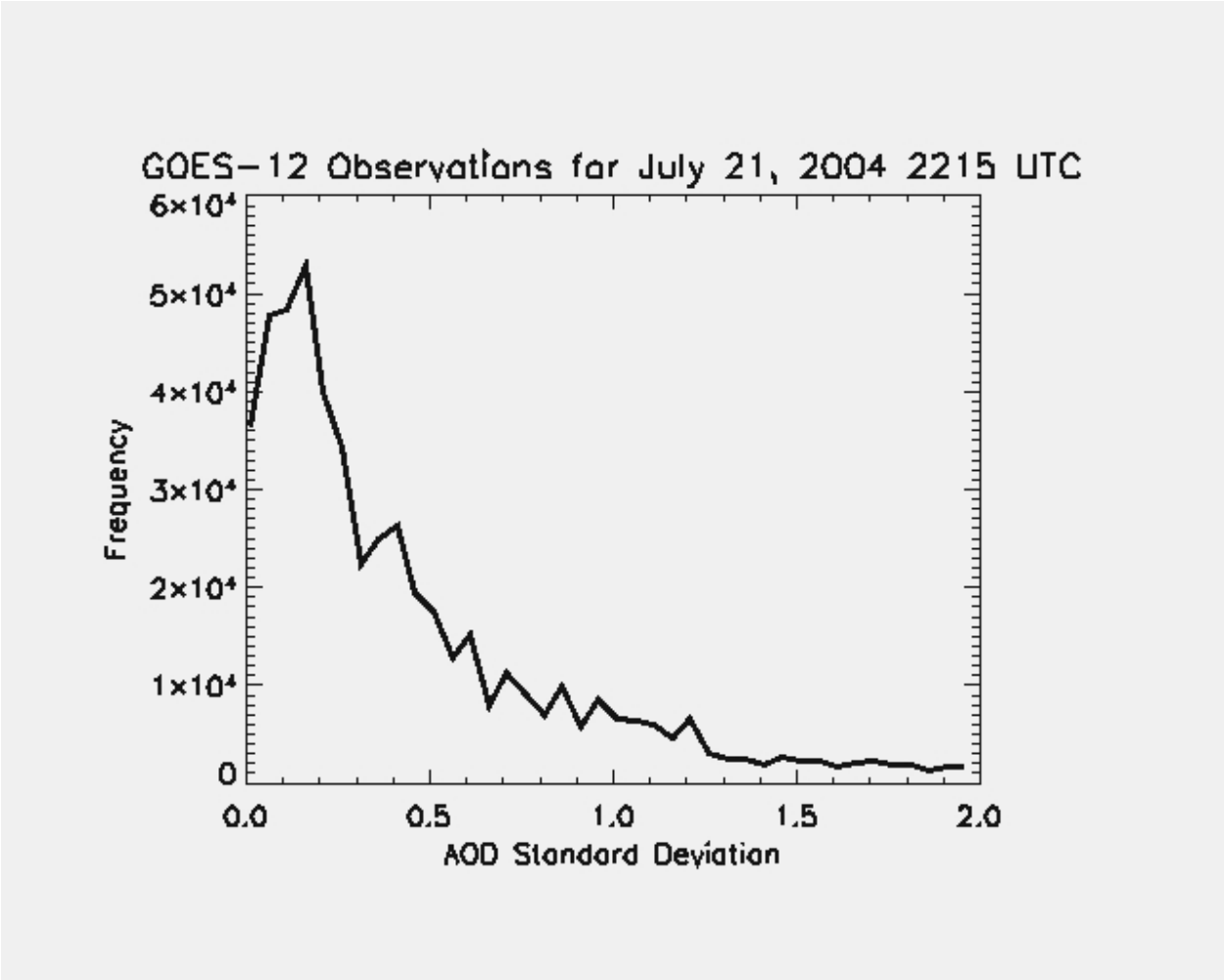

Figure 5: Frequency distribution of AOD standard deviation computed using AODs from 8 pixels in a 3 X 3 box surrounding a particular pixel. Data from July 21, 2004 2215Z were used in the analysis shown in the figure. Data from other days and other time periods show similar distribution.

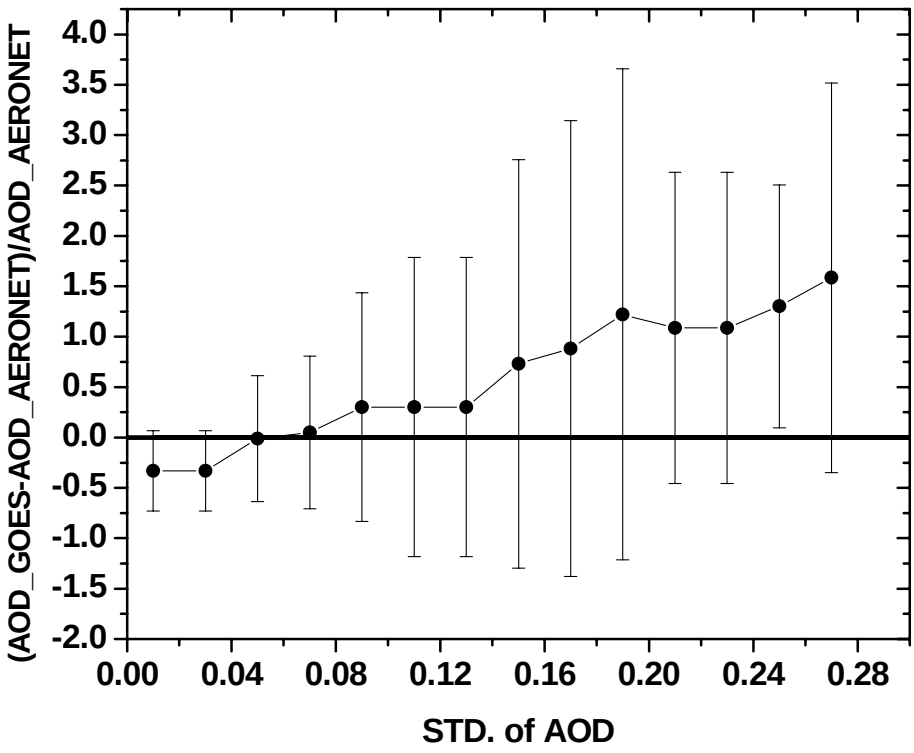

Figure 6: Relationship between GOES and AERONET AOD bias as a function of AOD standard deviation. AOD standard deviation was computed using AODs from 8 pixels surrounding a particular pixel. Bias increases with increasing AOD standard deviation indicating residual cloud contamination. The vertical bars are 1-σ variability over the mean AOD standard deviation.

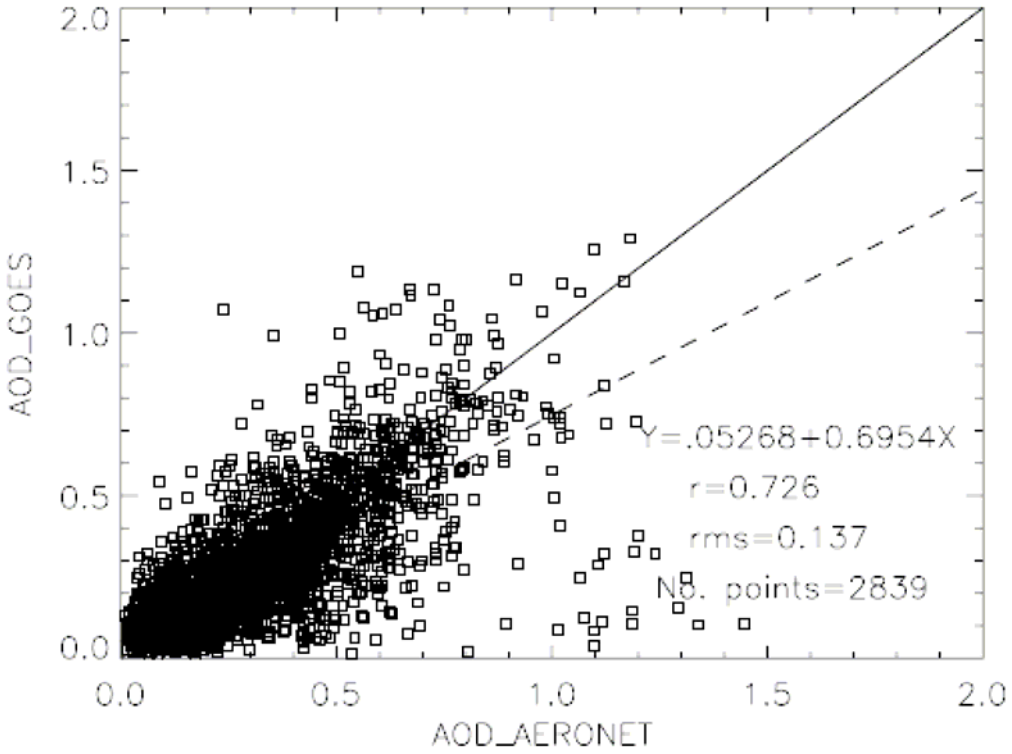

Figure 7: Correlation between GOES aerosol optical depth (AOD) and AODs measured from a network of 17 AERONET stations. Level 1.5 AERONET data were used. Matchup criteria were coincident measurements within 15 minutes. GOES AOD data were excluded if surface reflectance was smaller than 0.5% or greater than 15%, AOD standard deviation in 3 X 3 box was greater than 0.1, and number of cloud-free pixels in the 5 X 5 box were less than 25. Solid line is the 1:1 line and the dashed line is for the derived regression equation.

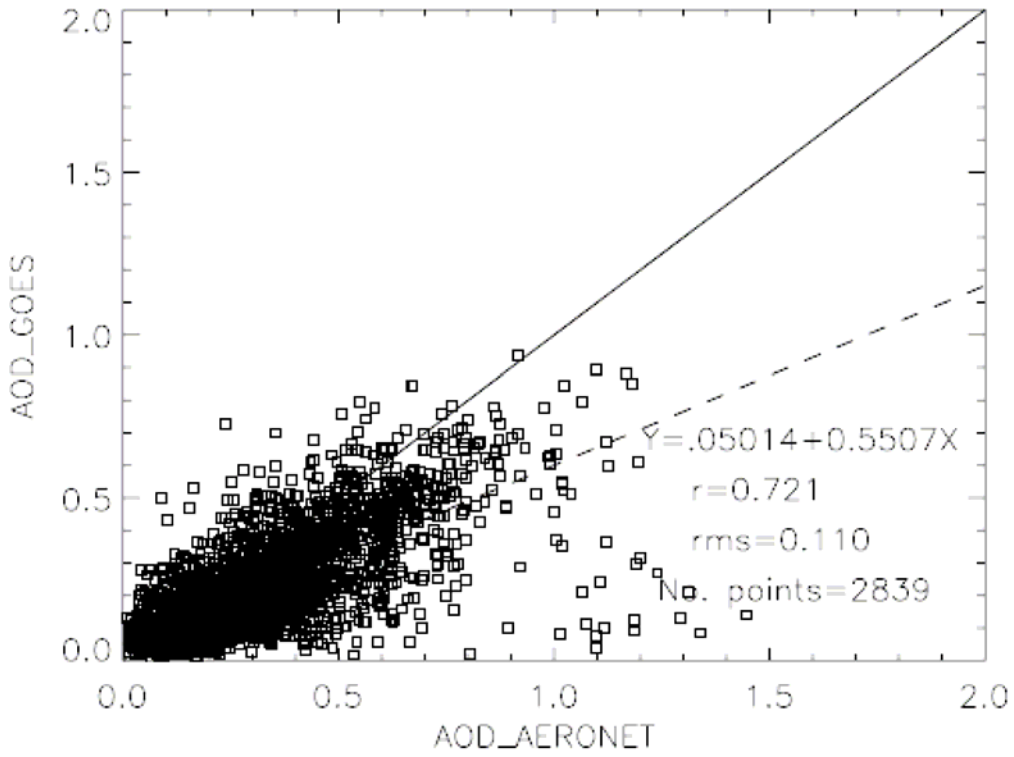

Figure 8: Same as figure 7 but for smoke aerosol model.

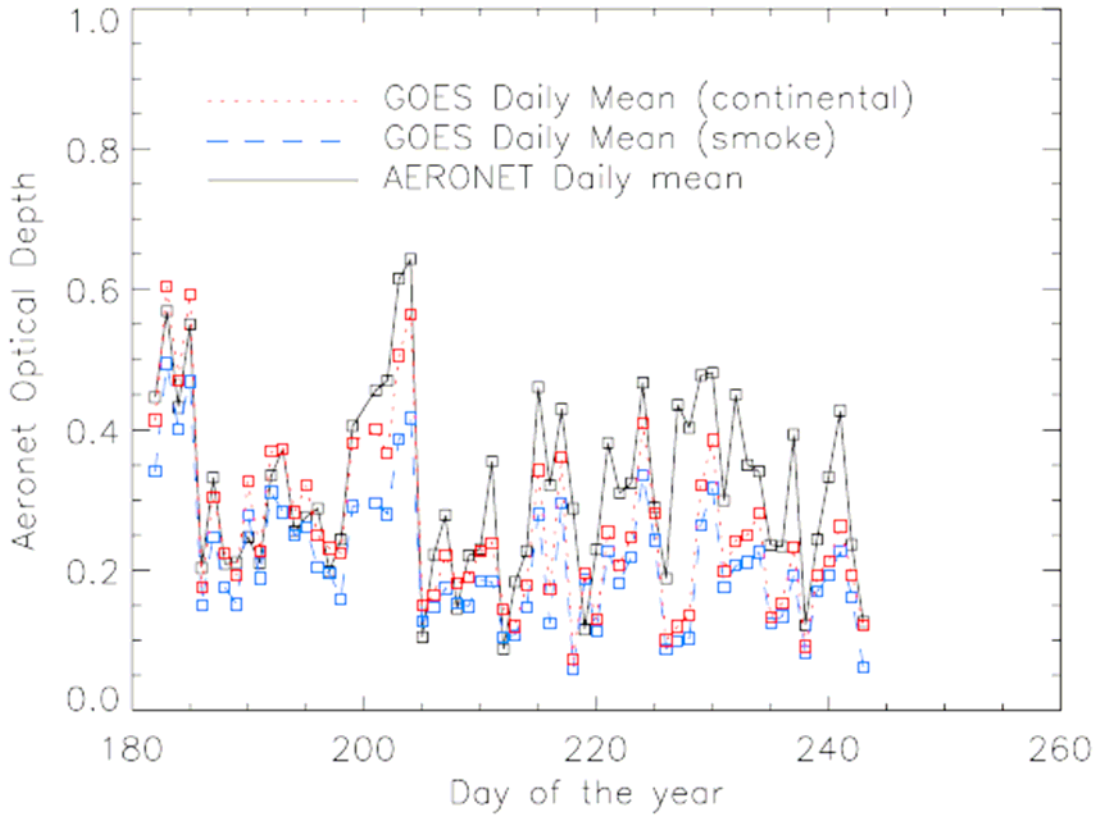

Figure 9: Time series of average daily mean GOES AOD overpass data from 17 AERONET stations. AERONET data are shown in black, GOES data processed with continental aerosol model in red, and GOES AOD data processed with smoke aerosol model in blue. Data begin on July 1, 2004 and end on August 31, 2004.

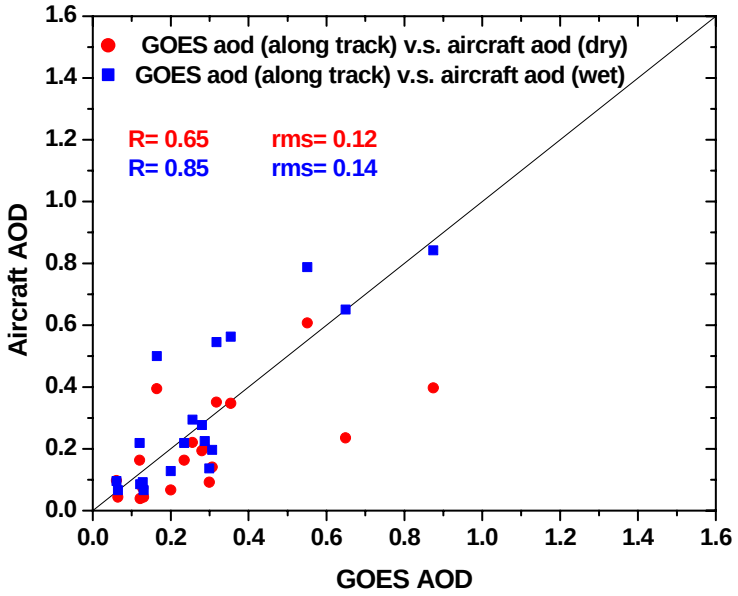

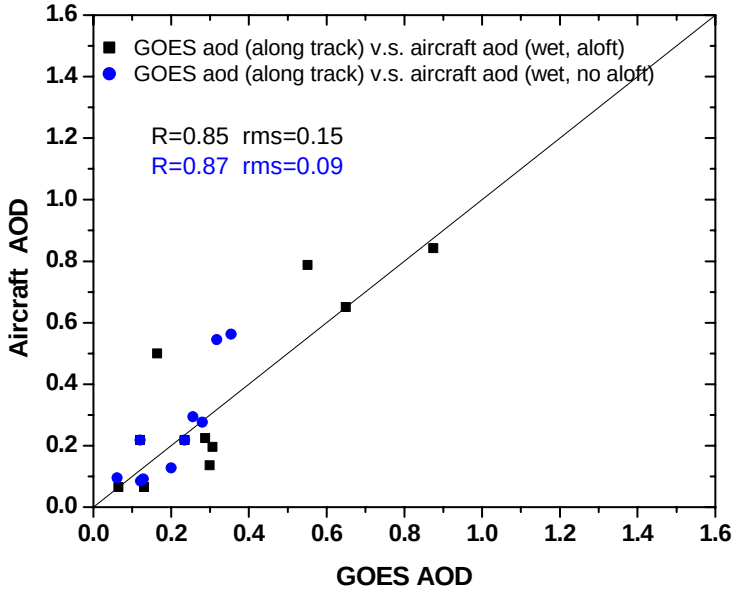

Figure 10: Ccorrelation between GOES and DC-8 aircraft measured AOD. Top panel is for wet and dry aerosols and bottom panel is for aerosols aloft vs not aloft.

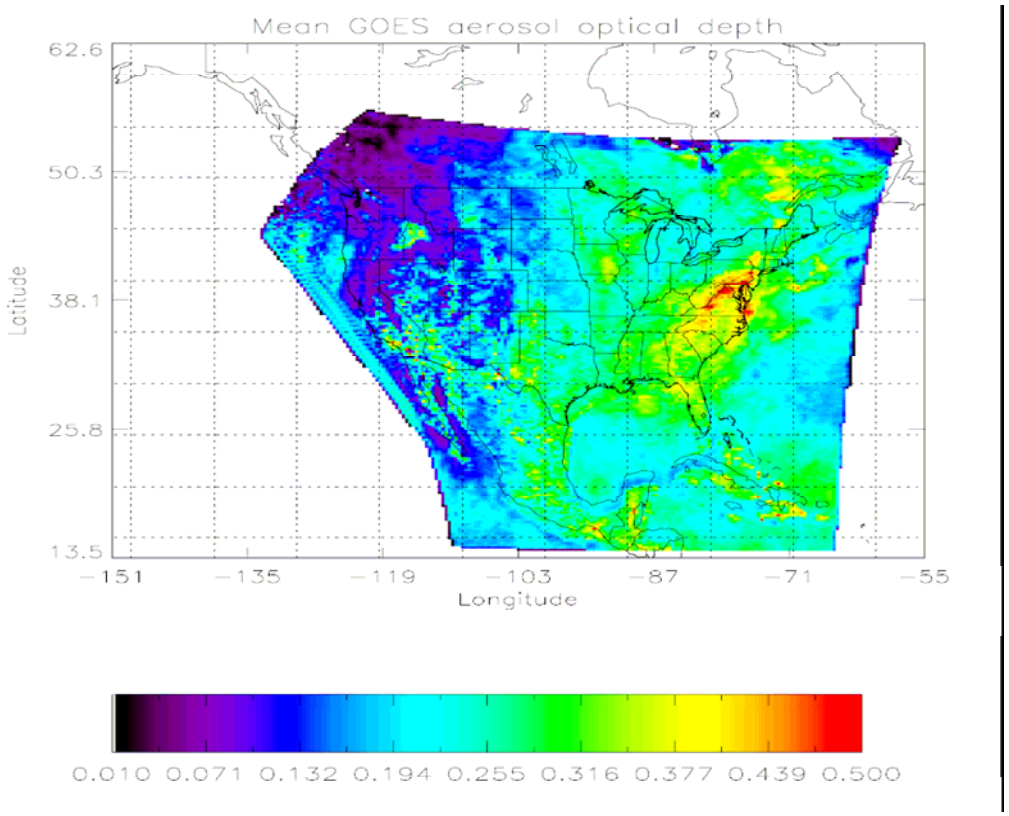

Figure 11: Mean aerosol optical depth for July – August, 2004 obtained from the visible channel of the GOES-12 Imager. AOD measurements are reported for 550 nm although the visible channel is a broad band covering 0.52 – 0.72 µm.

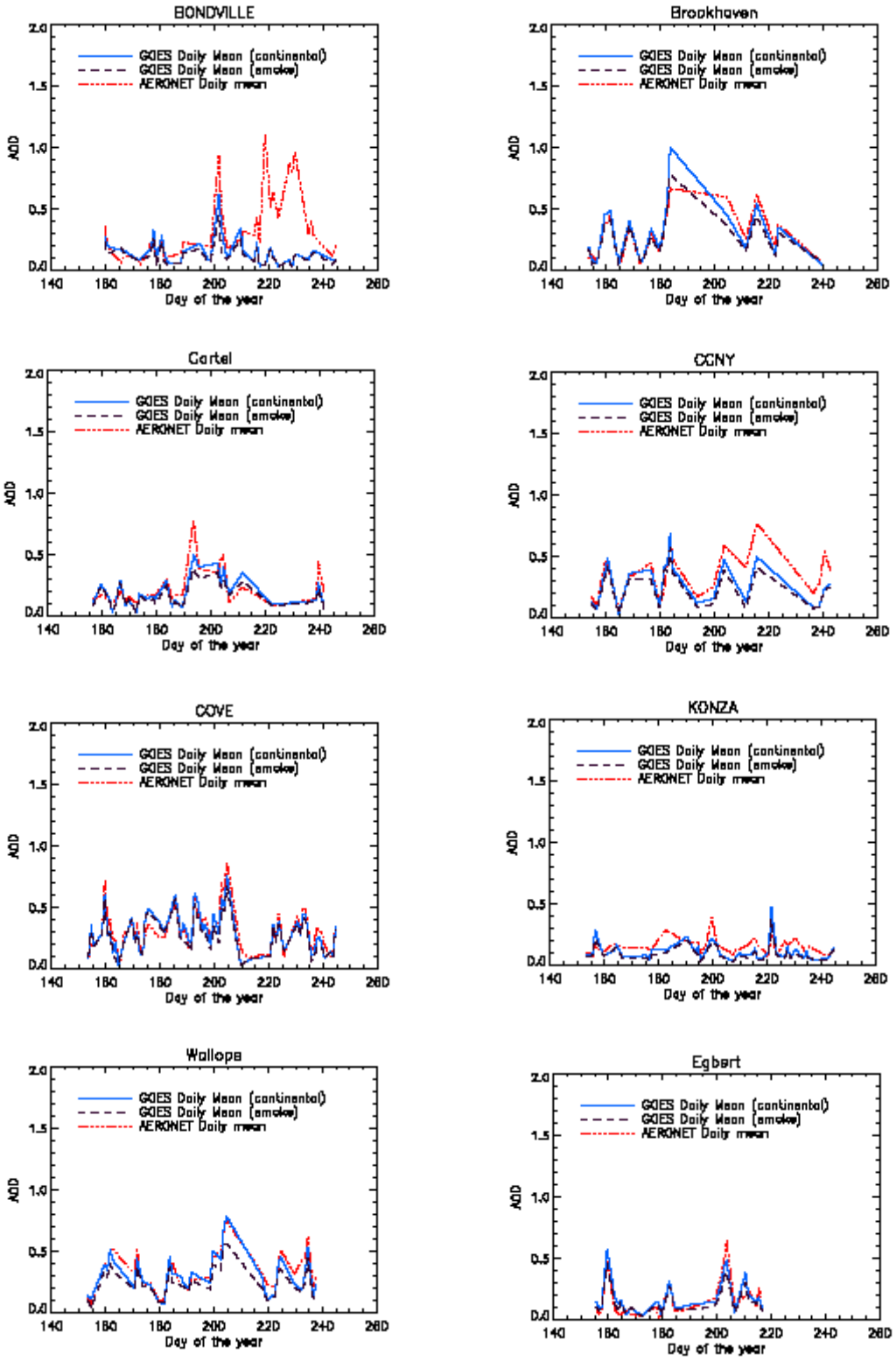

Figure 12: Time series of daily mean AOD from AERONET (red), GOES with continental aerosol model (blue), and GOES with smoke aerosol model (black) for eight different stations in the central and eastern U.S.